Effects and underlying cellular pathway involved in the impairment of the neurovascular unit following exposure of adult male mice to low doses of di(2-ethylhexyl) phthalate alone or in an environmental phthalate mixture

Delnia Ahmadpour, Sakina Mhaouty-Kodja, Valérie Grange-Messent

Title:

Effects and underlying cellular pathway involved in the impairment of the neurovascular unit following exposure of adult male mice to low doses of di(2-ethylhexyl) phthalate alone or in an environmental phthalate mixture

Authors:

Delnia Ahmadpour[1], Sakina Mhaouty-Kodja[1] and Valérie Grange-Messent[1*]

Affiliations:

[1]Sorbonne Université, CNRS, INSERM, Neuroscience Paris-Seine, Institut de Biologie Paris-Seine, 75005 Paris, France

***Corresponding author :**

Valérie Grange-Messent

Sorbonne Université, INSERM U1130, CNRS UMR 8246, Neuroscience Paris Seine, Institut de Biologie Paris-Seine, 7 quai St Bernard, 75005, Paris, France.

Tel: +33 1 44 27 36 57

Fax: +33 1 44 27 25 08

e.mail: valerie.messent@sorbonne-universite.fr

Abstract:

We have previously shown that adult male mice exposure to low doses of di(2-ethylhexyl)phthalate (DEHP) impacts the blood-brain barrier (BBB) integrity and surrounding parenchyma in the medial preoptic area (mPOA), a key hypothalamic area involved in the male sexual behavior. BBB leakage was associated with a decrease in the endothelial tight junction accessory protein, zona occludens-1, and caveolae protein Cav-1, added to an inflammatory profile including glial activation accompanied by enhanced expression of inducible nitric oxide synthase. As this failure of BBB functionality in the mPOA could participate, at least in part, in reported alteration of sexual behavior following DEHP exposure, we explored the cellular pathway connecting cerebral capillaries and neurons. Two-month-old C57BL/6J male mice were orally exposed for 6 weeks to DEHP alone (5 and 50 µg/kg/day) or to DEHP (5 µg/kg/day) in an environmental phthalate mixture. The presence of androgen receptor (AR) and estrogen receptor-α (ERα) were first evidenced in brain capillaries. Protein levels of AR but not of ERα were reduced in cerebral capillaries after phthalate exposure. The amounts of basement membrane and cell-matrix interaction components were decreased, while matrix metalloprotease MMP-2 and MMP-9 activities were increased. Fluorojade® labelling suggested that exposure to phthalates also lead to a neurodegenerative process in the mPOA. Altogether, the data suggest that environmental exposure to endocrine disruptors such as phthalates, could alter AR / Cav-1 interaction, impacting a Cav-1 / nitric oxide / MMP pathway. This would lead to disruption of the glio-neurovascular coupling which is essential to neuronal functioning.

Key words: androgen receptor, endocrine disruptors, hypothalamus, neurovascular unit, phthalates

Ethical statement:

The experiments have been reported in compliance with the Animal Research: Reporting in Vivo Experiments (ARRIVE) guidelines. All studies were performed in compliance with the National Institute of Health guidelines for the care and use of Laboratory Animals (NIH Guide) and French and European legal requirements (Decree 2010/63/UE). Experiments were performed, so as to minimize the numbers of animals used and their discomfort and were approved by the “Charles Darwin” Ethical committee (project number 01490-01).

Funding sources:

This work was supported by the Agence Nationale de la Recherche (Phtailure, 2018), France.

1 Introduction

The blood-brain barrier (BBB) is a highly regulated specific interface at the level of cerebral capillaries that maintains homeostasis of the central nervous system (CNS) to ensure neuronal activity underlying the regulation of all physiological functions (Daneman and Prat, 2015). BBB allows the control of substance delivery from the blood compartment to the brain parenchyma, as well as the elimination of compounds from the parenchyma to the blood flow. Cerebral endothelial cells strictly limit the passage across the BBB through inter-endothelial tight junction systems (TJs), selective transporters expressed on the luminal/abluminal side of endothelial cells as well as low rate of caveolae-mediated transcellular vesicular transport (Abbott et al., 2010). ECs are surrounded by a basement membrane, which is a unique form of the extracellular matrix (ECM). Basement membrane embedding pericytes also interacts with astrocytic end-feet (Correale and Villa, 2009), whose dynamic nature depends on its constitutive remodeling by several protease families, including the matrix metalloproteases (MMPs) (Rempe et al., 2016). The whole is called the neurovascular unit (NVU) and its integrity depends on the proper functioning of each element of this complex structure.

Cerebral vessels are target tissues for sex steroid hormones (Gonzales et al., 2007). In males, testosterone is the main sex steroid hormone. It activates androgen receptor (AR) and can be aromatized into neural estradiol, which then activates estrogen receptors (ER) α or ERβ (Mhaouty-Kodja, 2018). Testosterone was shown not only to promote cerebral angiogenesis and vasculature formation, but also to modulate the cerebrovascular function , such as the BBB integrity and function , and could prevent gliosis reaction and up-regulation of inflammatory components in male mice (Atallah et al., 2017), see for review, (Ahmadpour and Grange-Messent, 2020). Exposure to anti-androgenic compounds such as phthalates is known to trigger adverse health effects (Benjamin et al., 2017; Dombret et al., 2017; Zlatnik, 2016). These endocrine disruptors, which represent a high production volume, are used as plasticizers in plastic-based consumer products. Due to their extensive distribution in several daily life applications, they are widely propagated in our environment (Gao and Wen, 2016). Di(2-ethylhexyl) phthalate (DEHP) is the major phthalate family compound detected in the environment and it has been classified since 2000 by the European Union as a priority substance “presenting a significant risk to or via the aquatic environment” in the Water Framework Directive 2000/60/EC, which was updated in 2008 and 2013 (Directive 2013/39/EU of the European Parliament and of the Council of 12 August 2013). In addition to DEHP, other phthalates including diethyl phthalate (DEP), dibutyl

phthalate (DBP), butyl benzyl phthalate (BBP), and diisobutyl phthalate (DiBP) are commonly detected in the environment (Gao and Wen, 2016). Phthalates were mainly studied for their adverse effects on reproductive function in human or wild life (see for reviews, Mhaouty-Kodja et al., 2018; Rattan et al., 2017). However, the link between phthalate exposure and CNS function impairment has begun to emerge. The majority of *in vivo* studies have focused on the effects of perinatal exposure and the effects of adult exposure to low doses of phthalates are still largely under-explored.

We have recently shown that low doses of DEHP, alone or in an environmental phthalate mixture, have adverse effects on the NVU in adult male mice (Ahmadpour et al., 2021). Following adult exposure to DEHP alone at the tolerable daily intake (TDI) dose of 50 µg/kg/day (established by European Food Safety Authority (EFSA) in 2005 and 2019), or at the dose close to environmental exposure of 5 µg/kg/day or in a relevant mixture containing the most commonly phthalates detected in the environment listed above, BBB leakage was observed in the hypothalamic medial preoptic area (mPOA), the main cerebral area involved in the expression of male sexual behavior. This BBB leakage was sustained by a decrease of the levels of the tight junction's accessory protein Zonula Occludens (ZO-1) and of the caveolin-1 isoform protein (Cav-1), the main component of caveolae-transmembrane proteins. These features were accompanied by glial activation involving capillary-associated microglia and astrocytes (Ahmadpour et al., 2021). Moreover, such exposure to low doses of DEHP impaired sexual behavior of male mice through a down-regulation of neural AR expression in the mPOA without modification of circulating testosterone levels and/or the HPG axis (Dombret et al., 2017). Then, we suggested that failure of BBB functionality in the mPOA could participate, at least partly, in the reported-behavioral alteration following phthalate exposure (Ahmadpour et al., 2021).

Thus, our present work aims to explore the underlying cellular pathway which is damaged in those alterations of the NVU in the mPOA following adult exposure to low doses of phthalates.

To answer this question, experiments were performed using four experimental groups of adult C57BL/6J male mice exposed orally through contaminated diet to mimic the previous major route of exposure (Adam et al., 2021; Ahmadpour et al., 2021). The first three groups included males exposed for 6 weeks to the vehicle (control), DEHP at the TDI dose of 50 µg/kg/d, or DEHP at 5 µg/kg/d. The DEHP dose of 5 µg/kg/d is within the environmental exposure range. It induced sexual behavioral alterations in male mice following adult or pubertal exposure (Capela and Mhaouty-Kodja, 2021; Dombret et al., 2017). To mimic environmental co-exposure to phthalates (Dewalque et al.,

2014; Martine et al., 2013) , the fourth group of males was exposed to a phthalate mixture containing DEHP at 5 µg/kg/d, DBP at 0.5 µg/kg/d, BBP at 0.5 µg/kg/d, DiBP at 0.5 µg/kg/d and DEP at 0.25 µg/kg/d.

We first investigated the presence of AR and ERα in brain capillaries and more particularly in cerebral endothelial cells. Then, AR and ERα protein levels in cerebral capillaries were respectively compared after phthalate exposure. Proteolytic activity of matrix metalloproteases MMP-2 and MMP-9 and their respective protein levels were investigated. Basement membrane and cell-matrix interaction components were assessed in the four exposed groups. We also evaluated the effect of phthalate exposure on neurodegenerative process in this brain area.

2 Materials and methods

2.1 Ethical statement:

The experiments have been reported in compliance with the Animal Research: Reporting in Vivo Experiments (ARRIVE) guidelines. All studies were performed in compliance with the National Institute of Health guidelines for the care and use of Laboratory Animals (NIH Guide) and French and European legal requirements (Decree 2010/63/UE). Experiments were performed, so as to minimize the numbers of animals used and their discomfort and were approved by the “Charles Darwin” Ethical committee (project number 01490-01).

2.2 Animals

Male mice (n = 53 per treatment group) of the C57BL/6j strain (Janvier Labs, Le Genest-Saint-Isle, France) bred in our laboratory were housed in a conventional facility after weaning under a controlled photoperiod (12:12h light dark cycle-lights on at 1 p.m.), maintained at 22°C and relative humidity of 60 ± 10%, with free access to water and a standard diet (A03–10; Safe-diets, Augy, France). The mice were housed in nest-enriched polysulfone cages, with polysulfone bottles. Offspring were mixed at weaning to avoid potential litter effects, with no more than one male per litter per cage, and were allowed to grow to 8 weeks of age.

2.3 Phthalate exposure

Exposure to phthalates (Sigma Aldrich, Saint-Quentin Fallavier, France) was performed as recently described (Adam et al., 2021; Ahmadpour et al., 2021). The phthalates were first dissolved in absolute ethanol, then incorporated into food as previously detailed (Ahmadpour et al., 2021). Eight-week-old males were fed *ad libitum* for 6 weeks with chow reconstituted into pellets containing the vehicle i.e. ethanol and water (control group), DEHP (CAS 117-81-7)

at 50 or 5 µg/kg/d (DEHP-50 and DEHP-5 groups, respectively), or a phthalate mixture (Mix group) containing DEHP at 5 µg/kg/d, DBP (CAS 84-74-2) at 0.5 µg/kg/d, BBP (CAS 85-68-7) at 0.5 µg/kg/d, DiBP (CAS 84-69-5) at 0.5 µg/kg/d and DEP (CAS 84-66-2) at 0.25 µg/kg/d. The composition of the phthalate mixture was based on French and European studies showing an external co-exposure to these molecules and the presence of their metabolites in urinary samples (Dewalque et al., 2014; Martine et al., 2013). Mice were weighed weekly for the duration of the exposure and phthalate doses were adjusted to their body weights and calculated for a daily food intake of 5 g per animal (Cheema et al., 2019; Dombret et al., 2017). It has already been shown that such a phthalate exposure protocol had no effect on the body weight of individuals between the first and the last day of treatment (Ahmadpour et al., 2021).

Analyses were performed on 4 cohorts each comprising animals distributed equally between the 4 treatment groups. Briefly, two cohorts were used for immunohistochemistry, immunocytochemistry and microscopy studies. One was used for the capillary-enriched fraction procedure for western blot analysis and one for *in situ* zymography and Fluoro-Jade® C fluorescent investigation.

2.4 Electron microscope immunohistochemistry

Mice (n=3) were deeply anaesthetized with a lethal dose of pentobarbital (120 mg/kg, i.p.) and then transcardially perfused with 0.9% saline solution followed by a solution containing 0.2% glutaraldehyde, 4% paraformaldehyde in 0.1 M phosphate buffer (PB), pH 7.4. Brains were carefully removed, post-fixed with the same fixative solution overnight at 4°C and cut using a vibratome. Four to six floating frontal sections (40 µm thick) including the mPOA were treated by incubation in 0.1 M phosphate buffer saline (PBS) containing 1% bovine serum albumin (BSA) for 30 min at room temperature (RT) to block non-specific immune sites. AR or ERα proteins were detected using specific primary rabbit antibodies (Table 1) each diluted 1:200 in 0.1 M PBS-1% BSA, for 48 h at 4°C. After washes in PBS / BSA, immune complexes were fixed using a solution containing 0.1% glutaraldehyde in 0.1 M PB, pH 7.4 for 10 min at RT, and then detected by incubation for 4 h at RT in a solution containing 0.8 nm colloidal gold-labelled anti-rabbit IgG antibody (Biovalley, Marne la Vallée, France) diluted 1:100 in PBS-1%BSA. For intensification of the gold particles by silver, a commercial HQ Silver™ Enhancement kit (Nanoprobes, NY, USA) was used according to the recommendations of the manufacturer. At the end of the immunodetection procedure, half of the sections were observed under a Zeiss Axiovert 200 M light microscope (Göttingen, Germany) equipped with a black and white Axiocam MRm camera, while the other half of the labelled sections were washed in 0.1 M sodium cacodylate buffer,

post-fixed in 2% OsO_4 / 0.1 M sodium cacodylate buffer (v/v) for 1 h at RT, dehydrated through an alcohol ascending series and embedded in epoxy resin (Epoxy-Embedding Kit, Sigma Aldrich) and polymerized at 60°C for 48 h. Medial preoptic areas were selected and sectioned using an ultramicrotome (Leica Ultratcut). Ultrathin sections (70 nm) were contrasted with uranyl salts, and then observed under a transmission electron microscope (80–120 kV EM 912 Omega ZEISS) equipped with a digital camera (Veleta Olympus).

Table 1. Antibodies used in immunohistochemistry (IHC), transmission electron microcopy immunocytochemistry (TEM-ICC), and Western blot (WB)

Primary Antibody	**Host**	**Company**	**Catalog N°**	**Application**	**Dilution**
α-dystroglycan	Rabbit	Abcam	Ab151979	IHC-WB	1/300-1/500
AR	Rabbit	Abcam	Ab133273	WB	1/500
	Rabbit	Santa Cruz Biotechnology, Inc.	sc-816	TEM-ICC	1/200
Collagen IV	Rabbit	Sigma-Aldrich	SAB 4300738	WB	1/500
β-dystroglycan	Rabbit	Santa Cruz Biotechnology, Inc.	sc-28535	IHC - WB	1/200-1/300
Erα	Rabbit	Santa Cruz Biotechnology, Inc.	sc-542	WB	1/200
	Rabbit			TEM-ICC	1/200
GAPDH	Mouse	Santa Cruz Biotechnology, Inc.	sc-32233	WB	1/10000
β-integrin	Rabbit	Abclonal Technology	A11060	IHC-WB	1/100-1/500
Laminin α-1	Rabbit	Sigma-Aldrich	L9393	IHC - WB	1/200 - 1/100
MMP-2	Mouse	Santa Cruz Biotechnology, Inc.	sc-13594	WB	1/500
MMP-9	Mouse	Santa Cruz Biotechnology, Inc.	393859	WB	1/100

2.5 Transmission electron microscopy

For ultrastructural observation, mice (n=3 per treatment group) were deeply anaesthetized with a lethal dose of pentobarbital (120 mg/kg, i.p.) and were transcardially perfused with a 0.9% saline solution followed by a 2.5%

glutaraldehyde solution diluted in 0.1 M cacodylate buffer pH 7.4. Brains were removed and post-fixed in the same fixative solution overnight at 4°C, then in 2% OsO_4 / 0.1 M cacodylate buffer (v/v) for 1 h at RT. After washes in cacodylate buffer, four coronal sections including mPOA (100-µm thickness) were processed for embedding in epoxy resin as described above.

2.6 Fluorescent immunohistochemistry

The animals (n=5 per treatment group and per immuno-labelling) were deeply anaesthetized with a lethal dose of pentobarbital (120 mg/kg, i.p.) and then transcardially perfused with 0.9% saline solution followed by 4% paraformaldehyde solution diluted in 0.1 M PB pH 7.4. Brains were removed, post-fixed with the same fixative solution overnight at 4°C, and then cryoprotected with a 20% sucrose solution for 24 h at 4°C before freezing in isopentane (-30°C). Six to eight serial frozen sections (20 µm thick) including the mPOA were cut using a cryostat and collected on slides.

For immuno-labelling procedures, non-specific sites were blocked by incubating slide-mounted sections in PBS 1X, 1% BSA and 0.2% Triton X-100 for 1 h at RT. Then sections were incubated with primary antibodies (Table 1) overnight at 4° C diluted in the same phosphate buffer saline (PBS)/bovine serum albumin (BSA)/Triton X-100 solution. Immune complexes were revealed using secondary Alexa-conjugated anti-rabbit IgG (1:1000; Invitrogen, Villebon sur Yvette, France). Fluorescence was observed with a confocal microscope.

2.7 Confocal microscopy

Simple and multiple fluorescent labelling was visualized with a SP5 upright Leica confocal laser scanning microscope (Leica Microsystems) equipped with the Acousto-Optical Beam Splitter (AOBS) and using a 63x oil immersion objective. Alexa 488 was excited at 488nm and observed from 495 to 580 nm. Alexa 555 was excited at 555 nm and observed from 599 to 680 nm. The gain and offset for each photomultiplier were adjusted to optimize detection events. Images (1024x1024 pixels, 16 bits) were acquired sequentially between stacks to eliminate cross-over fluorescence. The frequency was set up at 400 Hz and the pinhole was set at 1 Airy. Each optical section (1 µm) was frame-averaged four times to enhance the signal/noise ratio. Overlays, projection of the z-stack files and quantification were performed using the Fiji software (NIH, USA). The presented pictures were the projection of 10–20 successive optical sections into one image, unless otherwise stated in the figure legend. Quantification of the

fluorescent density was performed on three sections sampled at the level of the mPOA (plate 30 of the Mouse Brain Atlas of Paxinos and Franklin 2001). The surfaces on which the fluorescence density quantifications were performed are indicated in the figure legends.

2.8 Western blot protein analysis using cerebral capillary-enriched factions

2.8.1 Cerebral capillary-enriched fraction procedure

Brains from 12 mice per treatment group were freshly removed, and two hypothalamus were pooled and placed quickly on ice (n = 6 per treatment group). Hypothalamic microvessels were harvested according to the previously described method (Atallah et al., 2017; Sandoval and Witt, 2011). Briefly, samples were homogenized in a pH 7.4 buffer containing 1% BSA, 2.7 mM KCl, 137 mM NaCl, 1.5 mM KH_2PO_4, 8 mM Na_2HPO_4, 1 mM $CaCl_2$, 0.5 mM $MgCl_2$, $6H_2O$, mM D-glucose, 1 mM sodium pyruvate, 1 M 4-(2-hydroxyethyl) piperazine-1-ethanesulfonic acid (HEPES). Homogenates were centrifuged in an equal volume of 30% Ficoll for 15 min at 4800g at 4°C, supernatants were aspirated and pellets suspended in isolation buffer without BSA and passed through a 70-µm nylon filter. Filtrates were centrifuged for 10 min at 4 °C at 3000g.

2.8.2 Protein extraction

Protein extraction from pellets of capillary-enriched fractions was performed with a RIPA buffer containing 50mM Tris—base (pH 7.2), 10 mM EDTA, 10 mM EGTA, 150 mM NaCl, 0.1% sodium dodecyl sulfate, 0.5% deoxycholate acid, 1% Triton X-100, and 1% protease inhibitor cocktail (Sigma Aldrich) and sonicated 10 times for 30 s. Homogenate samples were centrifuged at 13000 rpm for 13 min at 4°C and supernatants containing proteins were collected. The total protein concentration of each sample was determined using the Bradford Assay Kit (Thermo Scientific, Courtaboeuf-Villebon sur Yvette, France) according to the manufacturer's protocol. Protein extracts were stored at -20°C until further processing.

2.8.3 Electrophoresis and immunoblotting

Protein samples were denatured in Laemmli Buffer and heated at 95°C for 5 min. Electrophoretic migration of 10–20 µg of proteins was carried out on NuPAGE 4–12% Bis–Tris Gel (Invitrogen, Villebon sur Yvette, France). The resolved proteins were then electrotransferred onto pre-treated polyvinylidene difluoride (PVDF) membranes (Millipore, Molsheim, France).

Membranes with transferred proteins were blocked for 1 h at RT, with a solution of 5% non-fat milk diluted in PBS 1X with 0.2 % Tween, and then incubated with primary antibodies (Table 1) diluted in the same blocking solution overnight at 4°C. Primary antibody binding to blots was detected by incubation with respectively either secondary HRP–conjugated (1:5000; Jackson, Cambridgeshire, United Kingdom) or biotin–conjugated (1:2000; Vector, Burlingame, United States,) anti-rabbit or anti-mouse for 2 h, at RT, and then immune complexes were revealed by the SuperSignalTM West Pico or Femto Chemiluminescent Substrate kit (Thermo Scientific, Courtaboeuf-Villebon sur Yvette, France).

The signals were quantified by FiJi software (NIH, USA) and normalized to the value obtained for the corresponding housekeeper glyceraldehyde-3-phosphate dehydrogenase (GAPDH) protein band.

2.9 *In situ* Zymography

In situ zymography was used to check the gelatinase proteolytic activity of MMP-2 and MMP-9 in brain tissue using a commercial kit (EnzChek® Gelatinase/Collagenase Assay Kit, Thermo Fisher Scientific, Illkirch, France) following the manufacturer's instructions as previously described (Shu et al., 2015). Briefly, after a deep anaesthesia in mice (n= 4 per treatment group) with a lethal dose of pentobarbital (120 mg/kg, i.p.), brains were freshly removed and immediately frozen in isopentane (−30°C). Six to eight serial frozen sections (20-µm thickness) including the mPOA were cut and collected on slides. Four sections for each brain were processed for gelatinase activity and one section for each brain was processed for testing the specificity of the reaction using the metalloproteinase inhibitor, 1,10-phenanthroline, supplied in the kit. For gelatinase activity, cryosections were incubated in a humidity chamber for 1 h 30 at 37°C in the reaction buffer which contained 30 µg/ml of FITC-labelled DQ-gelatin. For gelatinase inhibitor assays, cryosections were incubated in a humidity chamber for 1 h 30 at 37°C in a reaction buffer which contained 0.5 mM 1,10-phenanthroline with the final substrate concentration of 30 µg/mL DQ-gelatin. Then, sections were rinsed and mounted with mounting medium, then imaged using a Hamamatsu NanoZoomer digital slide scanner 2.0 HT (Hamamatsu Photonics, Massy, France) and analysed with the corresponding NDP Viewer software (NDP.view2, Hamamatsu Photonics, Massy, France). The gelatin-FITC is cleaved by gelatinases, yielding peptides with green fluorescence intensity representative of net proteolytic activity.

2.10 Fluoro-Jade® C staining

To assess putative cellular damage induced by phthalate-generated BBB impairment, we used the Fluoro-Jade® C fluorescent marker which is commonly described as a useful specific tool to identify degenerating neurons, activated astrocytes, and microglia during a chronic neuronal degenerating process (Damjanac et al., 2007).

Fluoro-Jade® C staining of 20 µm-thickness frozen sections including mPOA was performed according to the manufacturer's instructions (Interchim, Montluçon, France). Briefly, animals (n=4 per treatment group) were deeply anaesthetized with a lethal dose of pentobarbital (120 mg/kg, i.p.) and slides bearing frozen cut tissue sections were first immersed in a basic alcohol solution consisting of 1% sodium hydroxide in 80% ethanol for 5 min at RT. Sections were rinsed for 2 min in 70% ethanol, for 2 min in distilled water, and then incubated in 0.06% potassium permanganate solution for 10 min. Following a 1-2 min water rinse, sections were transferred for 10 min to a 0.0004% solution containing Fluoro-Jade® C dissolved in 0.1% acetic acid. Sections were then rinsed through three changes of distilled water for 1 min per change, dried then cleared in xylene for at least 1 min. Fluorescence was analysed using a Hamamatsu slide scanner 2.0 HT, followed by analysis with the NDP Viewer software.

2.11 Statistical analysis

The four sample sizes corresponding to the vehicle-treated, DEHP-5 or DEHP-50 and phthalate mixture were equal. Normal distribution of the four groups was checked using the Shapiro-Wilk normality test then one-way ANOVA was used to analyse the main effects of exposure and Tukey tests were used for post hoc analyses to determine group differences. Differences were considered statistically significant if $p \leq 0.05$. In all figures, data are expressed as mean ± SEM for each group. In the main text of result section, the comparison between groups expressed in terms of percentage of the of the vehicle group (100%) in order to facilitate comparison.

3 Results

3.1 Effect of DEHP alone or in an environmental mixture on AR and ERα in mPOA cerebral capillaries

We first looked for the presence of AR and/or ERα proteins in capillaries located in the mPOA. Immunodetection using colloidal gold particles intensified by silver performed on brain sections from untreated mice, showed the presence of AR and ERα immunoreactivity in parenchymal cell nuclei in the hypothalamic mPOA, but also showed the presence of those sex steroid hormone receptors in capillary walls (Fig. 1 A and B). Ultrastructural observation

revealed their presence, at least partly, within cerebral endothelial cells, free in the cytoplasm or closely associated with plasma membrane or organelles such as mitochondria (Fig. 1C-F).

Then, we investigated whether the amounts of AR and/or ERα protein were affected in hypothalamic brain vessels of male mice exposed to DEHP alone or in a phthalate mixture. Data from Western blots performed on microvessel-enriched fractions obtained from the whole hypothalamus, highlighted a treatment effect on AR protein amount ($p \leq 0.05$), with a lower amount for both DEHP-50- and Mix-treated mice (-50 %, $p \leq 0.05$) (Fig. 1G). No significant effect of treatment to DEHP alone or in mixture was found on the amount of ERα in hypothalamic capillaries (Fig. 1H).

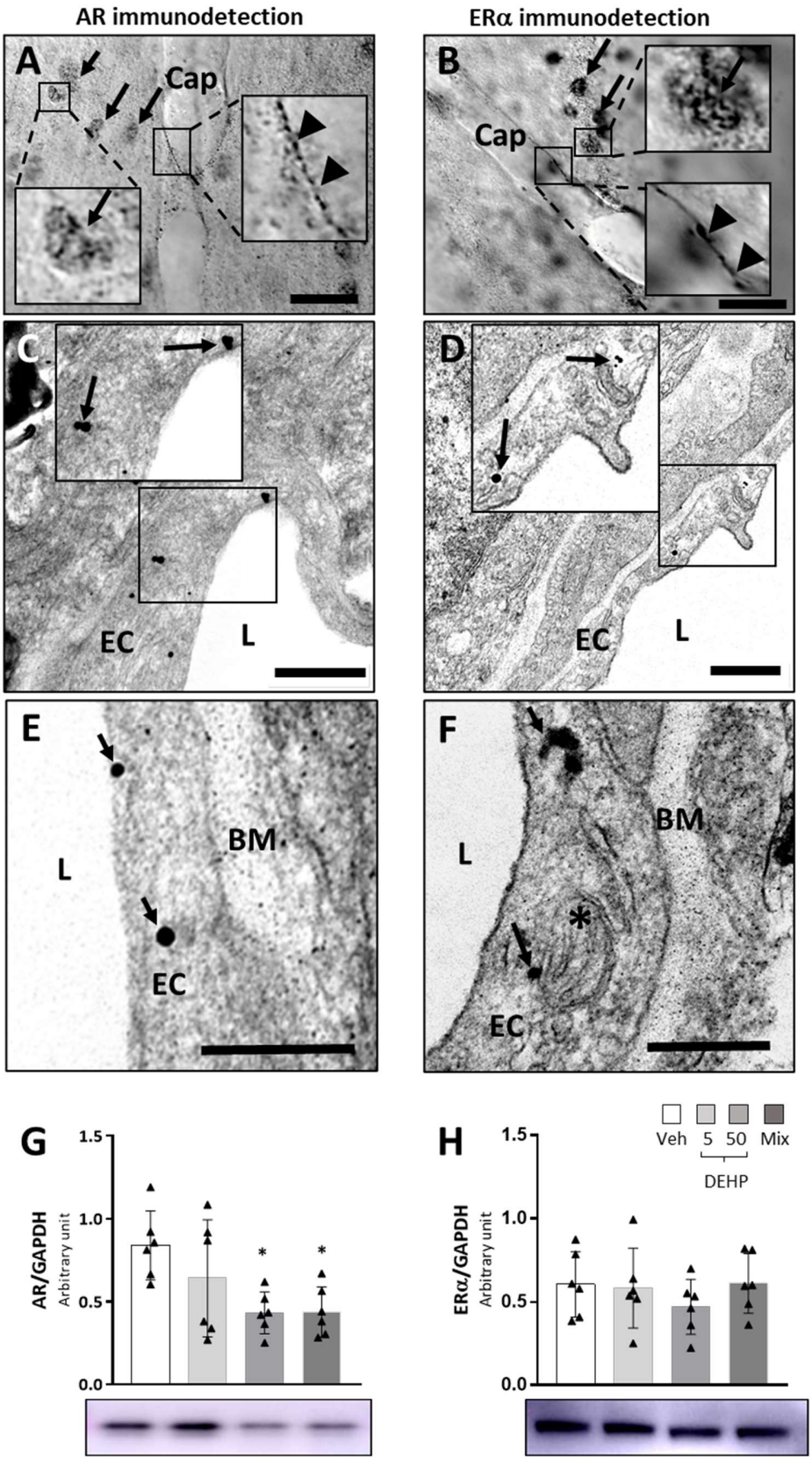
AR immunodetection
ERα immunodetection
A
Cap
B
Cap
C
EC
L
D
EC
L
E
BM
L
EC
F
BM
L
*
EC
G
AR/GAPDH
Arbitrary unit
1.5
1.0
0.5
0.0
*
*
H
Veh
5
50
Mix
DEHP
ERα/GAPDH
Arbitrary unit
1.5
1.0
0.5
0.0

Figure 1. Immunodetection of AR and ERα and effects of DEHP alone or in a phthalate mixture on their corresponding protein levels in cerebral capillaries of the hypothalamus in adult male mice.
Colloidal gold particles intensified by silver exhibit AR (A) and ERα (B). Arrows: Nuclear receptors, arrow heads: receptors in the blood vessel wall. Scale bar: Cap: blood capillary. Scale bar: 10 µm.
Ultrastructural observation using transmission electron microscopy show that both AR and ERα proteins are present in the cytoplasm of endothelial cells of capillaries in the mPOA. The presence of AR-immunoreactivity (C, D, arrows) is seen, at least partly, within cerebral endothelial cells, free in the cytoplasm or closely associated with the luminal plasma membrane. The cytoplasmic ERα-immunoreactivity (D, F, arrows) is detected in the cytoplasm, or associated to the outer membrane of mitochondria. Scale bar: 500 nm. BM: Basement membrane; EC: Endothelial cell; L: Lumen
*Western blot analysis (n = 6 per treatment group) of AR (G) and ERα (H) performed on microvessel-enriched fractions from hypothalamus of mice exposed to the Vehicle (Veh), DEHP at 5 µg/kg/d (DEHP-5), DEHP at 50 µg/kg/d (DEHP-50) or the phthalate mixture (Mix). All data are expressed as mean ± SEM. *p < 0.05 compared to the vehicle group. Data are normalized to GAPDH levels.*

3.2 Effects of DEHP alone or in an environmental mixture on metalloproteinase MMP-2 and MMP-9 activities and protein levels

MMPs such as gelatinases MMP-2 and MMP-9, are calcium-dependent zinc-containing endopeptidases. The proteolytic properties of MMPs determine the extent of ECM protein degradation and tissue remodeling surrounding cerebral capillaries. Here, we asked whether exposure to DEHP alone or in a mixture could lead to a dysregulation of MMP-2 and/or MMP-9 activity and/or affect their protein amounts.

An *in situ* gelatinase zymography study revealed higher levels of gelatinolytic activity in the mPOA after treatment ($p \leq 0.01$, Fig. 2A-D).

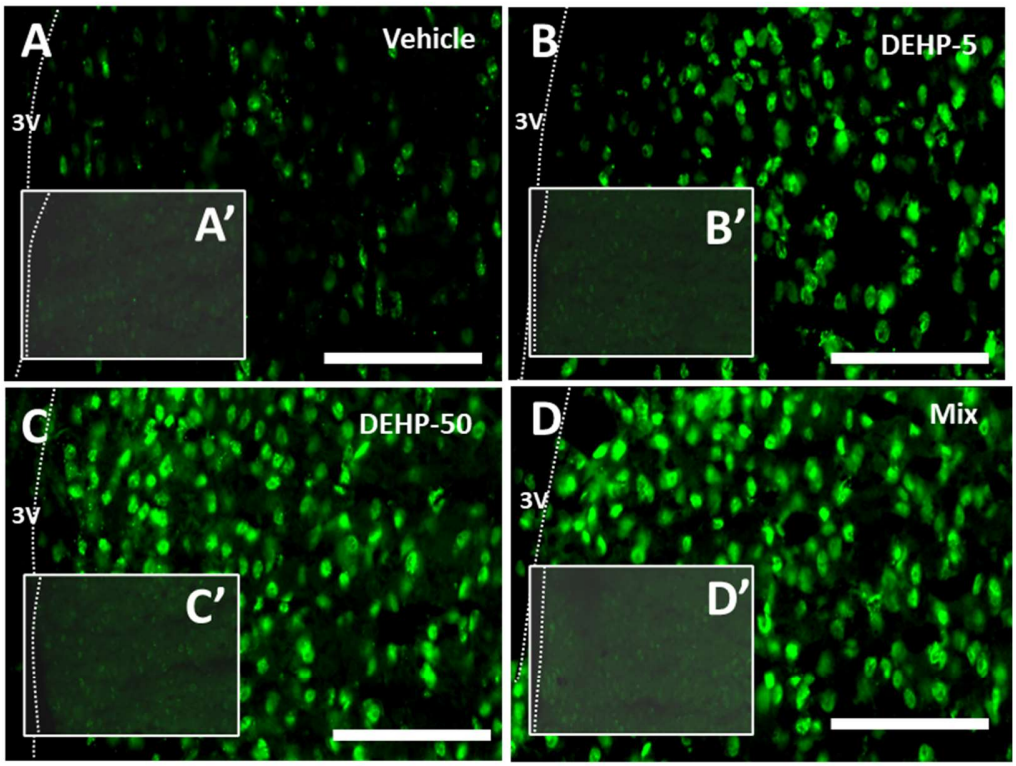
A
Vehicle
3V
A'
B
DEHP-5
3V
B'
C
DEHP-50
3V
C'
D
Mix
3V
D'

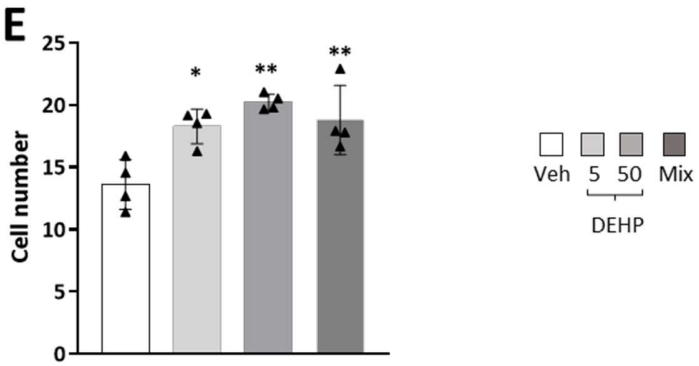
E
Cell number
25
20
15
10
5
0
*
**
**
Veh
5
50
Mix
DEHP

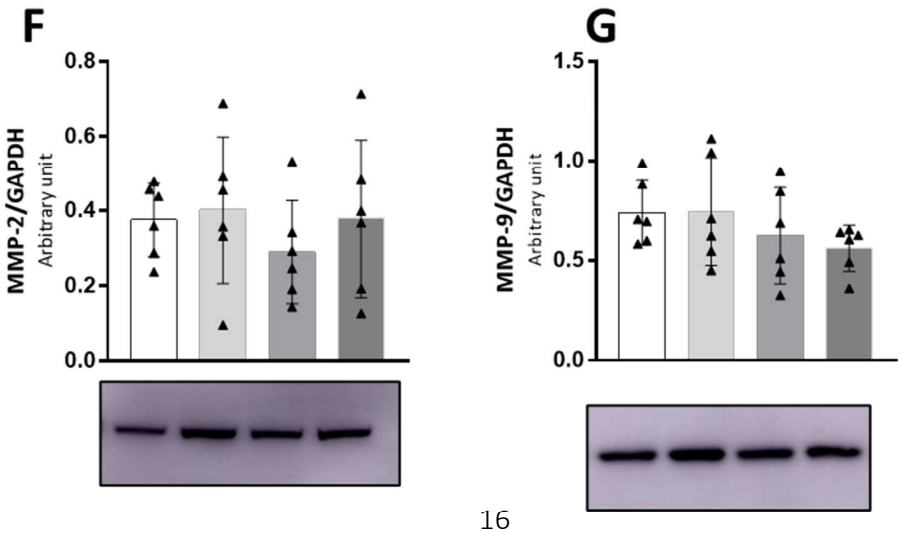
F
MMP-2/GAPDH
Arbitrary unit
0.8
0.6
0.4
0.2
0.0
G
MMP-9/GAPDH
Arbitrary unit
1.5
1.0
0.5
0.0

Figure 2. Effects of DEHP alone or in a phthalate mixture on MMP-2 and MMP-9 activities and their corresponding protein levels.

*Representative images of in situ zymography (n = 4 per treatment group, green fluorescence) without MMP inhibitor, in the mPOA of vehicle-treated (A), phthalate-treated mice by DEHP at 5 µg/kg/d (DEHP-5; B), DEHP at 50 µg/kg/d (DEHP-50; C) and phthalate mixture (Mix; D) or with the MMP inhibitor 1,10-phenanthroline, (A'-D'). Scale bar = 100 µm. The corresponding quantitative analysis of the gelatinase activity-labelling positive cell number (E, each dot represents the average of six to eight serial sections including the medial preoptic area per animal) and protein amount of MMP2 (F) or MMP9 (G) were based on Western blotting performed on microvessel-enriched fractions from the hypothalamus (n = 6 per treatment group). Data of Western blots were normalized to GAPDH levels. All data are expressed as mean ± SEM. *p < 0.05; **p < 0.01.*

Results showed a significant increase of the number of gelatinase-positive cells with more labelled cells for DEHP-5- (+ 34 %, $p \leq 0.05$), DEHP-50- (+ 48 %, $p \leq 0.01$) and Mix-treated mice (+ 38 %, $p \leq 0.01$) following post hoc analyses (Fig. 2E). To ensure the specificity of the signal, some representative sections from the four groups were treated with the MMP inhibitor, 1,10-phenanthroline, known to reversibly chelate zinc ions which are essential for MMP activity. Phenanthroline-treated sections showed an absence of signal (Fig. 2A'-D'). Western blot analysis performed on hypothalamic microvessel-enriched fractions showed no significant treatment effect on the amounts of either MMP-2 or MMP-9 (Fig. 2F and G, respectively).

3.3 Effects of DEHP alone or in an environmental mixture on the vascular basement membrane integrity

The basement membrane constitutes a continuous network of extracellular matrix, including, in particular, type IV-collagen and laminin. The integrity of the perivascular basement membrane is essential for BBB integrity. We investigated the distribution and amount of these major components, laminin α-1 and type IV-collagen α-1 (COL-IVα-1), assessed using immunofluorescence and Western blot analysis on hypothalamic microvessel-enriched fractions.

Fluorescent analysis revealed an effect of treatment ($p \leq 0.001$, Fig. 3A-B) on laminin α-1 immunoreactivity surrounding capillary walls and post hoc analyses showed a significant decrease for DEHP-5- (- 68 % $p \leq 0.0001$), DEHP-50- (-60 % $p \leq 0.0001$) and mixture-treated mice (-69 % $p \leq 0.0001$) in the mPOA. These results were confirmed by Western blot analysis performed on microvessel-enriched fractions showing a treatment effect in hypothalamic vessels ($p \leq 0.01$), with a decrease of -50 % ($p \leq 0.05$) in DEHP-5- and DEHP-50- groups, and -61 % ($p \leq 0.01$) in the mixture-group (Fig. 3C).

Western blot analysis also revealed an effect of treatment ($p \leq 0.01$) on the COL-IVα-1 amount with a significant decrease in the hypothalamus microvessel-enriched fraction of DEHP-5-, DEHP-50- and mixture-treated groups (-50 % $p \leq 0.05$ vs. vehicle) (Fig. 3D).

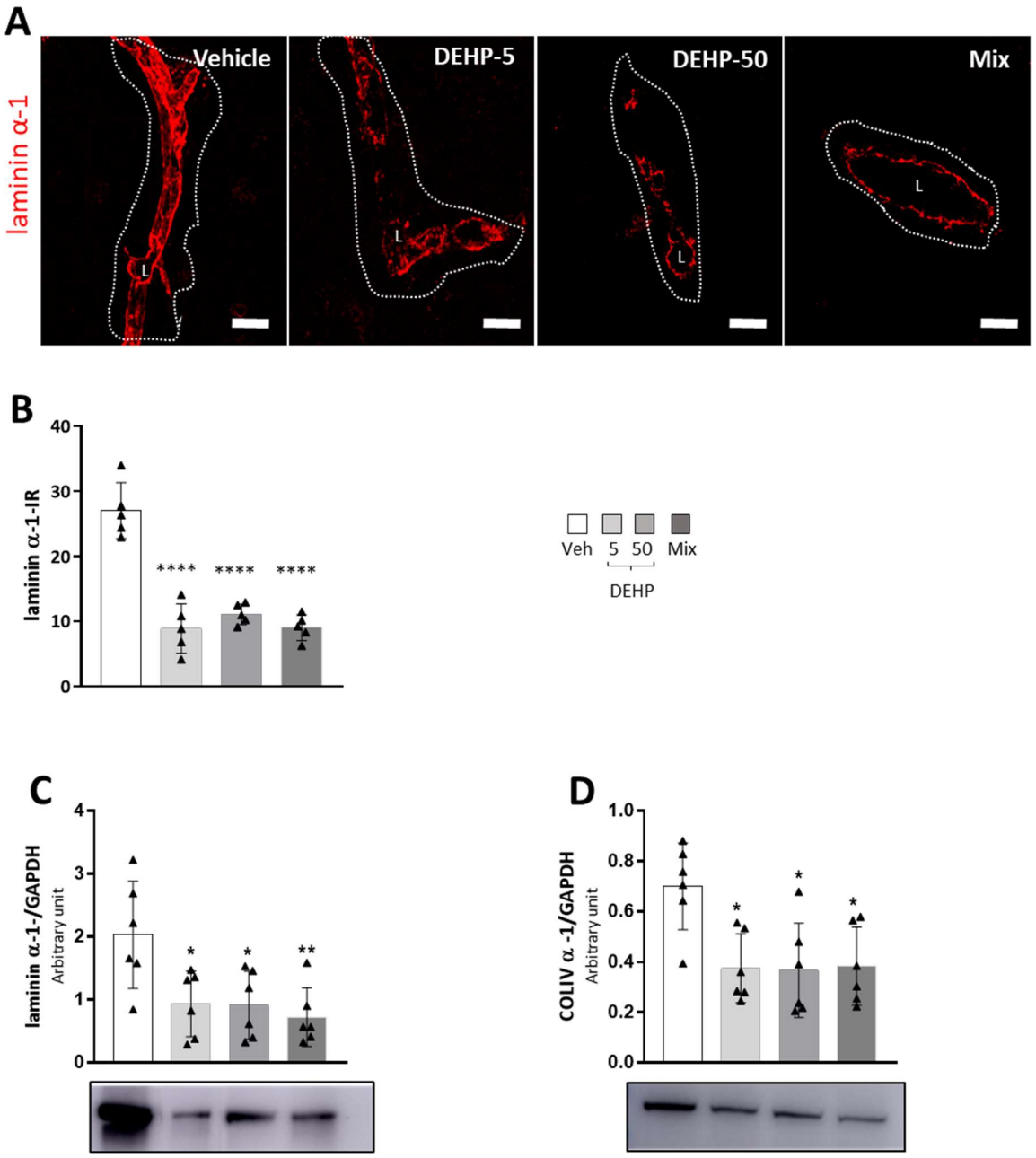

Figure 3. Effects of DEHP alone or in a phthalate mixture on proteins of the basement membrane surrounding endothelial cells of cerebral capillaries in the mPOA of male mice.

*Representative images (A) and corresponding quantitative analysis (B) of the six to eight serial sections for each brain examined by immunolabelling of laminin α-1 (red) in the mPOA of mice exposed to the vehicle (Veh), DEHP at 5 µg/kg/d (DEHP-5), DEHP at 50 µg/kg/d (DEHP-50), or phthalate mixture (Mix) (n = 5 per treatment group). Scale bar: 10 µm. L: Lumen. Quantifications of fluorescence density were measured over the surface delimited by the dotted lines and each dot on the graph B represents the average of the six to eight serial sections including the medial preoptic area per animal. Western blot analysis (n = 6 per treatment group) of laminin α-1 (C) and COLIV α-1 (D) performed on microvessel-enriched fractions from the hypothalamus. Data were normalized to GAPDH levels. All values represent mean ± SEM. *p < 0.05; **p < 0.01; ****p < 0.0001.*

Ultrastructural observation revealed a clean homogenous, compact and electron-dense perivascular basement membrane surrounding endothelial cells for the vehicle group (Fig. 4A), whereas this appeared fainter and sparser for DEHP-5-, DEHP-50- and mixture-treated mice, associated with an astrocyte end-feet swelling in contact with this basement membrane (Fig. 4B-D).

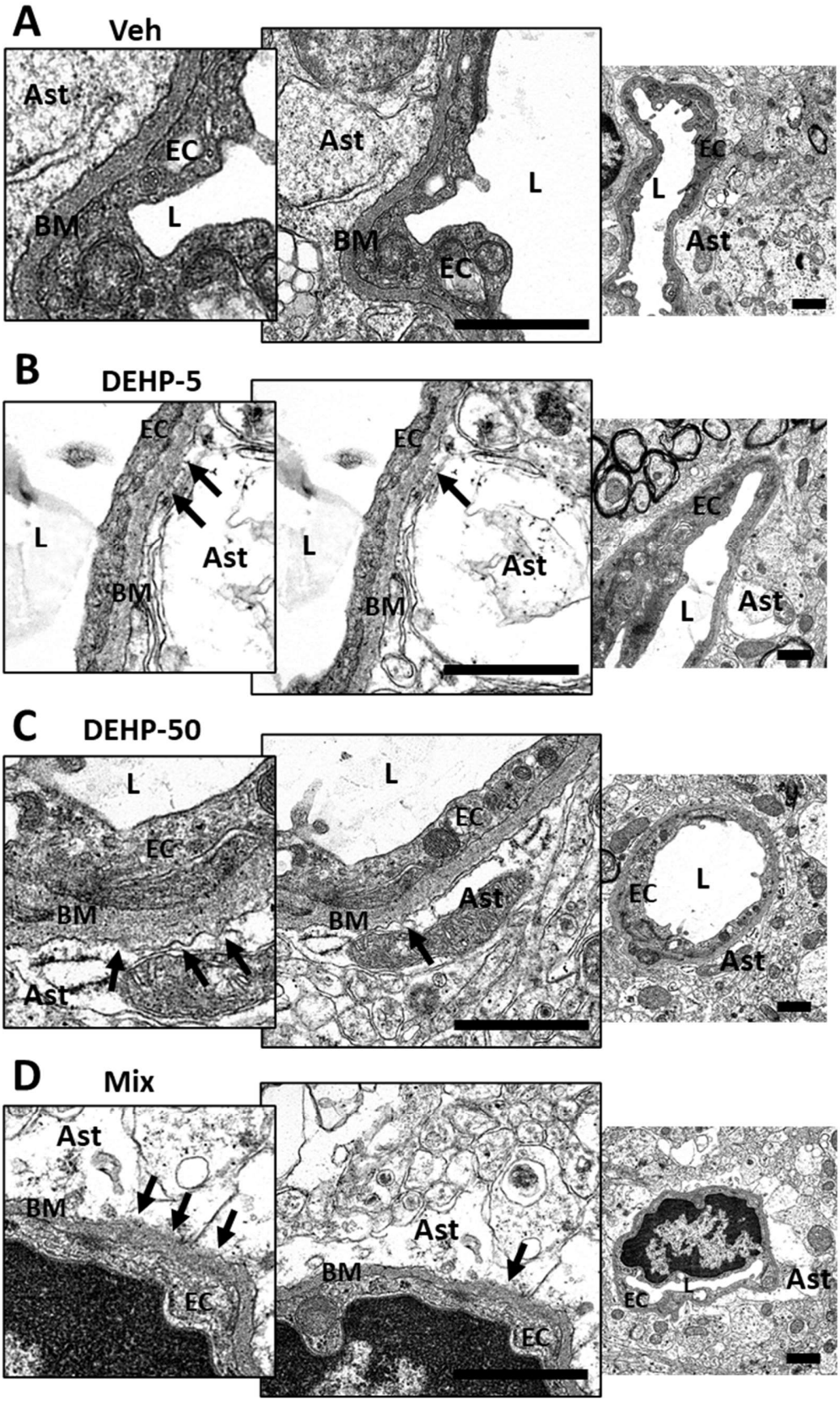
A
Veh
Ast
EC
L
BM
Ast
L
BM
EC
EC
L
Ast
B
DEHP-5
EC
L
Ast
BM
EC
L
Ast
BM
EC
L
Ast
C
DEHP-50
L
EC
BM
Ast
L
EC
BM
Ast
EC
L
Ast
D
Mix
Ast
BM
EC
Ast
BM
EC
EC
L
Ast

Figure 4. Ultrastrutural observation of the basement membrane surrounding endothelial cells of cerebral capillaries in the mPOA of male mice following exposure to DEHP alone or in a phthalate mixture.
Representative electron micrographs showing capillaries in the mPOA of mice exposed to vehicle (Veh; A), DEHP at 5 µg/kg/day (DEHP-5; B), DEHP at 50 µg/kg/day (DEHP-50; C), or phthalate mixture (Mix; D). (A) A clean homogenous, compact and electron-dense perivascular basement membrane surrounding endothelial cells is observed. (B, C, D) A faint, sparse and discontinuous (arrows) perivascular basement membrane is observed surrounding endothelial cells for DEHP-5, DEHP-50- and mixture-treated mice. A swelling of astrocyte end-feet in contact with this basement membrane is detected. Scale bar : 1 µm. Ast: Astrocyte end-foot; BM: Basement membrane; EC: Endothelial cell; L: Lumen.

3.4 Effects of DEHP alone or in an environmental mixture on extracellular matrix receptors

Dystroglycan and integrin represent the main receptors / adhesion proteins which are involved in cell-matrix interactions, thereby supporting BBB integrity. To determine if phthalates are involved in the impairment of cell-matrix interaction, we have investigated the distribution of β-dystroglycan using immunofluorescence and protein amounts of β-dystroglycan, α-dystroglycan and β-integrin. We carried out Western blot analysis on hypothalamus microvessel-enriched fractions.

A significant decrease ($p \leq 0.01$) of β-dystroglycan immunofluorescence density for DEHP-50-treated mice was observed in the mPOA area of brain sections (- 60%, $p < 0.05$ vs. vehicle) (Fig. 5A-B).

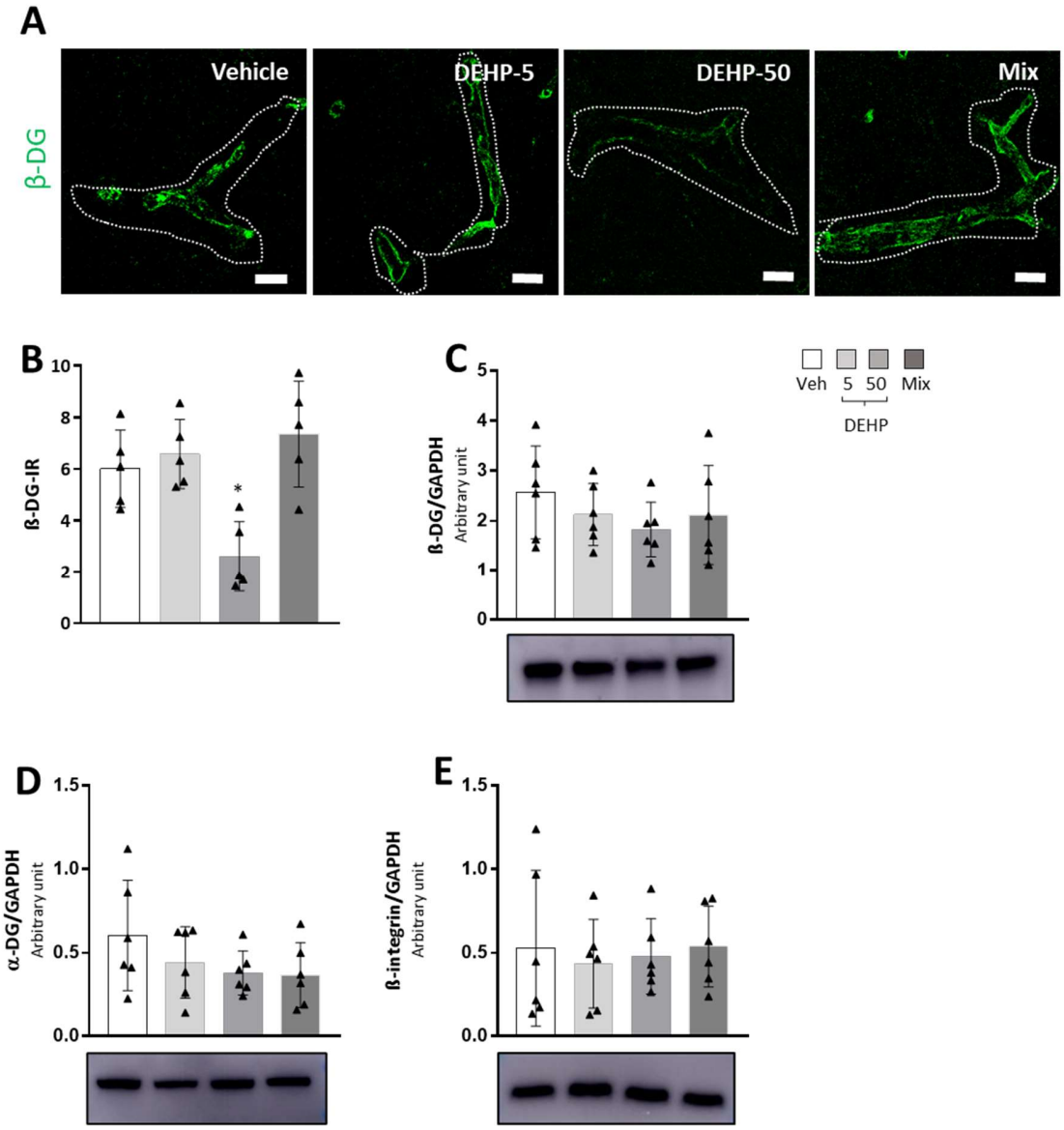

Figure 5. Effects of DEHP alone or in a phthalate mixture on extracellular matrix receptors.
*Representative images of the six to eight serial sections for each brain examined by immunolabelling of ß-DG (A) (green) and the corresponding quantitative analysis of the ß-DG immunoreactivity density (B) of mice exposed to the vehicle (Veh), DEHP at 5 µg/kg/d (DEHP-5), DEHP at 50 µg/kg/d (DEHP-50), or phthalate mixture (Mix) (n = 5 per treatment group). Scale bar: 10 µm. The dotted lines delimit the outer contour of the capillaries where fluorescence densities were quantified and each dot on the graph B represents the average of the six to eight serial sections including the medial preoptic area per animal. All values represent mean ± SEM. Western blot analysis of ß-DG (C), α-DG (D) and ß-integrin (E) were performed on microvessel-enriched fractions from the hypothalamus (n = 6 per treatment group). Data were normalized to GAPDH levels. All values represent mean ± SEM. *p < 0.05.*

No significant difference in the β-dystroglycan, α-dystroglycan or β-integrin protein amounts were measured in the hypothalamus microvessel-enriched fraction of treated mice (Fig. 5C-E).

3.5 Effects of DEHP alone or in an environmental mixture on neurodegenerative process

Both dysfunction of the BBB and neuroinflammatory status affect brain health, thus providing a starting point of neurodegenerative processes (Noe et al., 2020; Palmer, 2011).

The results showed an effect of treatment with a significant increase of the number of Fluoro-Jade® C -labelled cells ($p \leq 0.01$), highlighting more labelled cells for DEHP-5 (+84 %, $p \leq 0.05$), DEHP-50 (+89 %, $p \leq 0.01$) and Mix-treated mice (+74 %, $p \leq 0.05$) (Fig. 6A and B). Electron microscopy studies revealed the presence of degenerate cells for DEHP-5-, DEHP-50- and mixture-treated mice in the mPOA, which were morphologically identified as damaged neurons (Fig. 6C). Damaged neurons exhibited a very sparse electron-dense cytoplasm, intracellular edema with numerous intracytoplasmic vacuoles, dilation of the endoplasmic reticulum and destructured mitochondria.

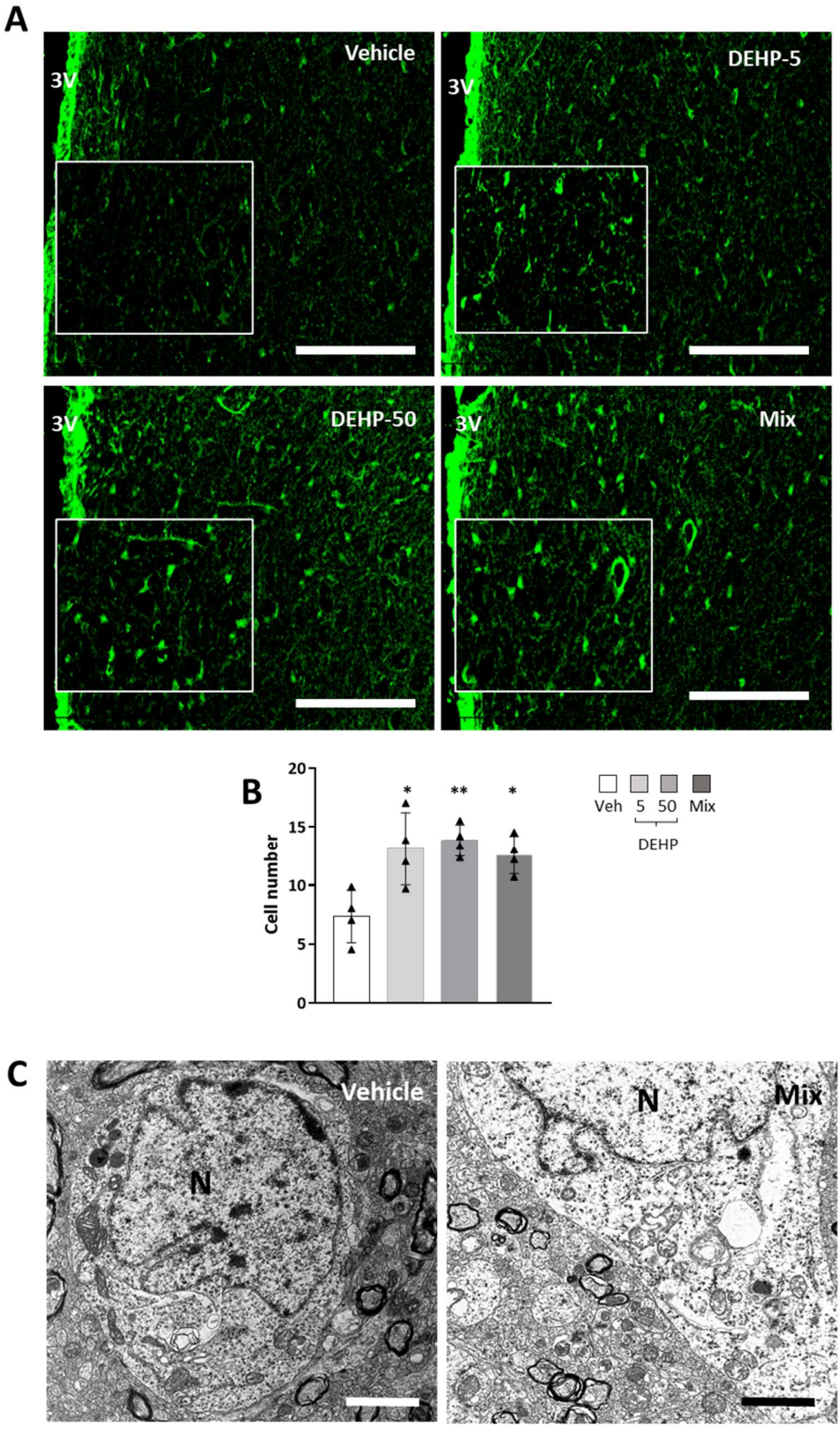
A
Vehicle
3V
DEHP-5
3V
DEHP-50
3V
Mix
3V
B
Cell number
20
15
10
5
0
*
**
*
Veh
5
50
Mix
DEHP
C
Vehicle
N
N
Mix

Figure 6. Effects of DEHP alone or in an environmental mixture in neurodegenerative process in the mPOA of male mice.

*Representative images of Fluoro-Jade® C fluorescent labelling (A) of the four serial sections for each brain examined in the mPOA of mice exposed to the vehicle (Veh), DEHP at 5 µg/kg/d (DEHP-5), DEHP at 50 µg/kg/d (DEHP-50), or phthalate mixture (Mix) (n = 4 per treatment group) and corresponding quantitative analysis of the number positive cells for Fluoro-Jade® C labelling (B, each dot represents the average of the six to eight serial sections including the medial preoptic area per animal). All values represent mean ± SEM. *p < 0.05; **p < 0.01. Scale bar = 100 µm. (C) Representative electron micrographs showing an intact neuron in the mPOA of mice exposed to vehicle (Veh; left panel), and a damaged neuron in the mPOA of mice exposed to the phthalate mixture (Mix; right panel). Scale bar = 2 µm.*

4 Discussion

Our previous study demonstrated that DEHP exposure alone or in an environmental mixture is associated with an impairment of the NVU in androgen-sensitive brain regions including the hypothalamic mPOA (Ahmadpour et al., 2021). The present study aimed to explore the mechanisms involved in these phthalate-induced alterations.

The anti-androgenic action of low doses of phthalates during adult exposure has been previously evidenced in male mice by a downregulation of neural AR, but not ERα, in the hypothalamic median preoptic nucleus of male mice leading to sexual behavior disruption (Dombret et al., 2017). ARs and ERs are commonly detected in the nuclei of neural cells including neurons and astrocytes (Lorenz et al., 2005) especially in the hypothalamic mPOA in male mice (DonCarlos et al., 2006). Our present data show for the first time to our knowledge, the presence of cytoplasmic immunoreactive AR and ERα proteins in the capillary wall of adult male mice, suggesting that they could also be targets for anti-androgenic endocrine disruptors. We show that exposure to DEHP alone at 50 µg / kg / day or at 5 µg / kg / day or in a phthalate mixture affects the protein levels of the AR but not of ERα in the capillaries of the hypothalamus in male mice, confirming the anti-androgenic action of low doses of phthalates also in brain capillaries. AR and ER respective signaling pathways modulate several CNS activities through genomic but also non-genomic actions (Patchev et al., 2004). Thus, our results highlight a possible involvement of the non-genomic AR signaling pathway which could lead to a rapid vascular response as a target of anti-androgenic compounds in this androgen-sensitive brain area.

Non-genomic AR activity may ultimately serve to influence AR genomic activity (Bennett et al., 2010). The AR interacts with a large number of co-regulators which function as transactivation chaperones (see for review, (Bennett et al., 2010). For instance, among these AR co-regulators, caveolin-1 isoform protein (Cav-1), an integral caveolae structural protein present in endothelial cells and astrocytes, is a well-known AR co-activator through its transient interaction

with Cav-1 (Ikezu et al., 1998). This interaction may be necessary prior to non-genomic AR activity originating from caveolae structures (Lu et al., 2001). We have previously shown that adult exposure to low doses of DEHP alone or in an environmental phthalate mixture triggers a significant high decrease of Cav-1 in the hypothalamus (Ahmadpour et al., 2021). Phthalate-induced downregulation of AR and/or Cav-1 in brain capillaries could lead to a reduced interaction between Cav-1 and AR and so to a lower AR transactivation.

Besides that, Cav-1 protein inhibits nitric oxide (NO)-mediated MMP activities and Cav-1 protein deficiency increases gelatinase activity such as matrix metalloproteinases 2 and 9 (MMP-2, MMP-9) (Gu et al., 2012). Our present results show a significant increase of the MMP-2 and MMP-9 gelatinase activity in the hypothalamic mPOA following exposure to DEHP at 5 µg / kg / day alone or in a phthalate mixture and to DEHP at 50 µg / kg / day. In addition, similar phthalate exposure induced an increase of inducible nitric oxide synthase (iNOS) protein in the mPOA (Ahmadpour et al., 2021), suggesting an increase of NO production. Thus, the increase of the activity of MMPs demonstrated here could be due, at least partly, to the decrease in Cav-1 protein levels leading to a disinhibition of NOS and an increase of NO production. Our results are in accordance with those suggesting that the Cav-1 / nitric oxide / MMP pathway could be considered as a therapeutic target to ensure vascular protection (Chen et al., 2018). Furthermore, gelatinases MMP-2 and MMP-9 have been shown to mediate the rearrangement and degradation of several endothelial tight junction proteins including ZO-1 (Bauer et al., 2010; Higashida et al., 2011). In our previous work, we have also demonstrated that the increased BBB permeability coincided with the reduction of the tight junction accessory protein ZO-1 level in hypothalamus microvessels following exposure to DEHP at 5 µg / kg / day alone or in a phthalate mixture and to DEHP at 50 µg / kg / day (Ahmadpour et al., 2021). This increased gelatinolytic activity that we report in the present study, could mediate the rearrangement and/or degradation of ZO-1, leading to BBB leakage (Bauer et al., 2010; Higashida et al., 2011).

Metalloproteases such as gelatinases have been shown to contribute to BBB leakage and neuroinflammation by mediating the degradation of the extracellular matrix surrounding cerebral blood vessels (Rempe et al., 2016; Thomsen et al., 2017). Basement membrane proteins laminin and collagen IV, synthesized predominantly by brain microvascular endothelial cells, pericytes and astrocytes, play a pivotal role in vascular integrity including BBB maintain (Chen et al., 2013; Jeanne et al., 2015). In the mPOA, exposure to DEHP alone or in an environmental phthalate mixture induced a decreased immunoreactivity for laminin α-1 and decreased protein levels of both

laminin α-1 and collagen IV based on Western blot analysis performed on hypothalamic microvessel-enriched fractions. Thus, the increase of the gelatinase activity following phthalate exposure may lead to an alteration / remodeling of the ECM surrounding brain capillaries in this hypothalamic brain area. This could be also responsible for the neurovascular unit impairment.

The BBB integrity is mainly ensured by cell-basement membrane interactions involving, at least partly, the cellular adhesion receptors such as the β-integrin protein and the dystroglycan complex (Baeten and Akassoglou, 2011). In the brain, different neuronal subtypes and glial cells express dystroglycan (Zaccaria et al., 2001) and integrin is expressed by all the components of the NVU (Baeten and Akassoglou, 2011). The β-integrin receptor mediates anchoring of brain endothelial cells to extracellular matrix components including laminin and Col-IV (Edwards and Bix, 2018; Engelhardt, 2011) but is not affected by phthalate exposure. The dystroglycan complex is constituted by two subunits α and β formed by proteolytic cleavage of a common precursor, and is expressed in perivascular astrocytes, neurons, and endothelial cells. The α-dystroglycan is an extracellular subunit binding to extracellular matrix components such as laminin, whereas β-dystroglycan is a transmembrane protein that anchors α-dystroglycan and actin cytoskeleton, as well as proteins involved in the formation of membrane microdomains such as caveolae (Montanaro and Carbonetto, 2003; Sharma et al., 2010). Our present data show that the alteration of the basement membrane in the mPOA was concomitant to a decrease of β-dystroglycan following exposure to DEHP at 50 µg/ kg / day. The glio-vascular connection which is mediated by the basement membrane, play a crucial role in the integrity, formation and maintenance of the BBB (Ezan et al., 2012; Wolburg et al., 2009). In our previous study (Ahmadpour et al., 2021), we observed a decreased protein amounts of the astrocytic GFAP in the hypothalamic capillary-enriched fractions which could correspond to a retraction in the astrocyte end-feet, a clue to astrocyte-capillaries decoupling. It may originate from basement membrane impairment and basal membrane receptor alteration caused by MMP-2 and MMP-9 activation. Dystroglycan can be altered by MMPs, thus amplifying several pathogenic states (Hayward and Gordon, 2018) and causing BBB dysfunction (Zhang et al., 2019). β-dystroglycan and tight junction-associated ZO-1 protein interact together through the actin cytoskeleton. In addition, dystroglycan participates in astrocyte-mediated fluid homeostasis through involvement in polarization and distribution of the water-channel protein aquaporin-4 in perivascular astrocytic end-feet (Noell et al., 2011).

Astrocytes also support neurons in the vicinity of the endothelial cells by regulating of blood flow, fluid, ion, pH, neurotransmitter homeostasis, and energy and metabolism (Sofroniew and Vinters, 2010). Given their strategic location and their function, simultaneous communication with neurons and microvessels, astrocyte morphological and/or function changes may precede or be accompanied by neuronal damage (Zlokovic, 2008). Neurodegeneration in the mPOA was higher in treated mice than in vehicle-treated mice. Thus, astrocyte activation, leading to inflammatory mediator production, and MMP activation, leading to neurovascular unit impairment, could be responsible of the present observed neuronal degenerative process in the mPOA (Rempe et al., 2016), as inflammatory mediators can serve as signaling molecules to induce neurodegeneration (Noe et al., 2020).

5 Conclusion

In conclusion, a decrease in the interaction between AR and Cav-1 protein in brain capillaries, a consequence of a decrease in their levels induced by phthalate exposure, leads to the activation of gelatinases which, in turn, generates alteration of the basement membrane and cell-matrix interactions (Table 2), resulting in disruption of the neurovascular unit and neuronal damages. This lower AR / Cav-1 interaction would lead to an excessive amount of NO produced following phthalate-induced disinhibition of iNOS in astrocyte end-feet associated with capillaries (Ahmadpour et al., 2021). NO is a signaling free radical involved, among others, in most pathologic features associated with a neurodegenerative and neuroinflammatory status (Saha and Pahan, 2006).

Table 2: Synthesis of the effects of an oral exposure during adulhood to low doses of DEHP alone or in a phthalate mixture in male mice on the neurovascular unit in the hypothalamus mPOA

Sex steroid receptors in capillaries	
AR	present; decreased: DEHP-50 and Mix
ERα	present; no significant change
Gelatinases MMP-2 and MMP-9	
Activity	increased: DEHP-5, DEHP-50 and Mix
Protein level	no significant change
Basement membrane components	
Laminin	decreased: DEHP-5, DEHP-50 and Mix

Collagen IV	decreased: DEHP-5, DEHP-50 and Mix
Cell / matrix interaction receptors	
α-dystroglycan	no significant change
β-dystroglycan	decreased: DEHP-50
β-intergrin	no significant change
Neurodegenerescence	increased: DEHP-5, DEHP-50 and Mix

The proposed AR-mediated cellular pathway (Graphical abstract) would lead to a failure of the glio-neurovascular coupling which could be involved in the phthalate-induced impairment of male sexual behavior. These data also raise the question of the involvement of endocrine disruptors with anti-androgenic activity in the onset and/or progression of neurodegenerative processes and consequently of complications of many brain diseases and injuries (Baeten and Akassoglou, 2011; Liebner et al., 2018; Sweeney et al., 2018). This, together with the tight regulation exerted by testosterone, allowed us to suggest that exposure to endocrine disruptors such as phthalates may be considered as an environmental risk factor for the cerebrovascular function.

Conflict of interest:

The authors declare that they have no known competing financial interests or personal relationships that could have appeared to influence the work reported in this paper.

Acknwolegments:

This work was supported by the Agence Nationale de la Recherche (Phtailure, 2018), France. We thank the rodent facility of the Institut de Biologie Paris-Seine (IBPS, Paris, France) for taking care of the animals and the IBPS Imaging facility.

Author contributions

Delnia Ahmadpour: Investigation, Formal analysis, Writing-original draft**. Valérie Grange-Messent**: Conceptualization, Supervision, Writing-review & editing. **Sakina Mhaouty-Kodja**: Funding acquisition, Review & editing.

6 References

Abbott, N.J., Patabendige, A.A.K., Dolman, D.E.M., Yusof, S.R., Begley, D.J., 2010. Structure and function of the blood–brain barrier. Neurobiol. Dis., Special Issue: Blood Brain Barrier 37, 13–25. https://doi.org/10.1016/j.nbd.2009.07.030

Adam, N., Brusamonti, L., Mhaouty-Kodja, S., 2021. Exposure of Adult Female Mice to Low Doses of di(2-ethylhexyl) Phthalate Alone or in an Environmental Phthalate Mixture: Evaluation of Reproductive Behavior and Underlying Neural Mechanisms. Environ. Health Perspect. 129. https://doi.org/10.1289/EHP7662

Ahmadpour, D., Grange-Messent, V., 2020. Involvement of testosterone signaling in the integrity of the neurovascular unit in the male: review of evidence, contradictions and hypothesis. Neuroendocrinology. https://doi.org/10.1159/000509218

Ahmadpour, D., Mhaouty-Kodja, S., Grange-Messent, V., 2021. Disruption of the blood-brain barrier and its close environment following adult exposure to low doses of di(2-ethylhexyl)phthalate alone or in an environmental phthalate mixture in male mice. Chemosphere 282, 131013. https://doi.org/10.1016/j.chemosphere.2021.131013

Atallah, A., Mhaouty-Kodja, S., Grange-Messent, V., 2017. Chronic depletion of gonadal testosterone leads to blood–brain barrier dysfunction and inflammation in male mice. J. Cereb. Blood Flow Metab. 37, 3161–3175. https://doi.org/10.1177/0271678X16683961

Baeten, K.M., Akassoglou, K., 2011. Extracellular matrix and matrix receptors in blood-brain barrier formation and stroke. Dev. Neurobiol. 71, 1018–1039. https://doi.org/10.1002/dneu.20954

Bauer, A.T., Bürgers, H.F., Rabie, T., Marti, H.H., 2010. Matrix metalloproteinase-9 mediates hypoxia-induced vascular leakage in the brain via tight junction rearrangement. J. Cereb. Blood Flow Metab. Off. J. Int. Soc. Cereb. Blood Flow Metab. 30, 837–848. https://doi.org/10.1038/jcbfm.2009.248

Benjamin, S., Masai, E., Kamimura, N., Takahashi, K., Anderson, R.C., Faisal, P.A., 2017. Phthalates impact human health: Epidemiological evidences and plausible mechanism of action. J. Hazard. Mater. 340, 360–383. https://doi.org/10.1016/j.jhazmat.2017.06.036

Bennett, N.C., Gardiner, R.A., Hooper, J.D., Johnson, D.W., Gobe, G.C., 2010. Molecular cell biology of androgen receptor signalling. Int. J. Biochem. Cell Biol. 42, 813–827. https://doi.org/10.1016/j.biocel.2009.11.013

Capela, D., Mhaouty-Kodja, S., 2021. Effects of pubertal exposure to low doses of di-(2-ethylexyl)phthalate on reproductive behaviors in male mice. Chemosphere 263, 128191. https://doi.org/10.1016/j.chemosphere.2020.128191

Cheema, U.B., Most, E., Eder, K., Ringseis, R., 2019. Effect of lifelong carnitine supplementation on plasma and tissue carnitine status, hepatic lipid metabolism and stress signalling pathways and skeletal muscle transcriptome in mice at advanced age. Br. J. Nutr. 121, 1323–1333. https://doi.org/10.1017/S0007114519000709

Chen, H., Chen, X., Li, W., Shen, J., 2018. Targeting RNS/caveolin-1/MMP signaling cascades to protect against cerebral ischemia-reperfusion injuries: potential application for drug discovery. Acta Pharmacol. Sin. 39, 669–682. https://doi.org/10.1038/aps.2018.27

Chen, Z.-L., Yao, Y., Norris, E.H., Kruyer, A., Jno-Charles, O., Akhmerov, A., Strickland, S., 2013. Ablation of astrocytic laminin impairs vascular smooth muscle cell function and leads to hemorrhagic stroke. J. Cell Biol. 202, 381–395. https://doi.org/10.1083/jcb.201212032

Correale, J., Villa, A., 2009. Cellular elements of the blood-brain barrier. Neurochem. Res. 34, 2067–2077. https://doi.org/10.1007/s11064-009-0081-y

Damjanac, M., Rioux Bilan, A., Barrier, L., Pontcharraud, R., Anne, C., Hugon, J., Page, G., 2007. Fluoro-Jade B staining as useful tool to identify activated microglia and astrocytes in a mouse transgenic model of Alzheimer's disease. Brain Res. 1128, 40–49. https://doi.org/10.1016/j.brainres.2006.05.050

Daneman, R., Prat, A., 2015. The blood-brain barrier. Cold Spring Harb. Perspect. Biol. 7, a020412. https://doi.org/10.1101/cshperspect.a020412

Dewalque, L., Charlier, C., Pirard, C., 2014. Estimated daily intake and cumulative risk assessment of phthalate diesters in a Belgian general population. Toxicol. Lett. 231, 161–168. https://doi.org/10.1016/j.toxlet.2014.06.028

Dombret, C., Capela, D., Poissenot, K., Parmentier, C., Bergsten, E., Pionneau, C., Chardonnet, S., Hardin-Pouzet, H., Grange-Messent, V., Keller, M., Franceschini, I., Mhaouty-Kodja, S., 2017. Neural Mechanisms Underlying the Disruption of Male Courtship Behavior by Adult Exposure to Di(2-ethylhexyl) Phthalate in Mice. Environ. Health Perspect. 125, 097001. https://doi.org/10.1289/EHP1443

DonCarlos, L.L., Sarkey, S., Lorenz, B., Azcoitia, I., Garcia-Ovejero, D., Huppenbauer, C., Garcia-Segura, L.-M., 2006. Novel cellular phenotypes and subcellular sites for androgen action in the forebrain. Neuroscience 138, 801–807. https://doi.org/10.1016/j.neuroscience.2005.06.020

Edwards, D.N., Bix, G.J., 2018. Roles of blood-brain barrier integrins and extracellular matrix in stroke. Am. J. Physiol.-Cell Physiol. 316, C252–C263. https://doi.org/10.1152/ajpcell.00151.2018

Engelhardt, B., 2011. β1-Integrin/matrix interactions support blood–brain barrier integrity. J. Cereb. Blood Flow Metab. 31, 1969–1971. https://doi.org/10.1038/jcbfm.2011.98

Ezan, P., André, P., Cisternino, S., Saubaméa, B., Boulay, A.-C., Doutremer, S., Thomas, M.-A., Quenech'du, N., Giaume, C., Cohen-Salmon, M., 2012. Deletion of astroglial connexins weakens the blood–brain barrier. J. Cereb. Blood Flow Metab. 32, 1457–1467. https://doi.org/10.1038/jcbfm.2012.45

Gao, D.-W., Wen, Z.-D., 2016. Phthalate esters in the environment: A critical review of their occurrence, biodegradation, and removal during wastewater treatment processes. Sci. Total Environ. 541, 986–1001. https://doi.org/10.1016/j.scitotenv.2015.09.148

Gonzales, R.J., Ansar, S., Duckles, S.P., Krause, D.N., 2007. Androgenic/Estrogenic Balance in the Male Rat Cerebral Circulation: Metabolic Enzymes and Sex Steroid Receptors. J. Cereb. Blood Flow Metab. 27, 1841–1852. https://doi.org/10.1038/sj.jcbfm.9600483

Gu, Y., Zheng, G., Xu, M., Li, Y., Chen, X., Zhu, W., Tong, Y., Chung, S.K., Liu, K.J., Shen, J., 2012. Caveolin-1 regulates nitric oxide-mediated matrix metalloproteinases activity and blood-brain barrier permeability in focal cerebral ischemia and reperfusion injury. J. Neurochem. 120, 147–156. https://doi.org/10.1111/j.1471-4159.2011.07542.x

Hayward, A.N., Gordon, W.R., 2018. Dystroglycan proteolysis is conformationally-regulated and disrupted by disease-associated mutations. bioRxiv 279315. https://doi.org/10.1101/279315

Higashida, T., Kreipke, C.W., Rafols, J.A., Peng, C., Schafer, S., Schafer, P., Ding, J.Y., Dornbos, D., Li, X., Guthikonda, M., Rossi, N.F., Ding, Y., 2011. The role of hypoxia-inducible factor-1α, aquaporin-4, and matrix metalloproteinase-9 in blood-brain barrier disruption and brain edema after traumatic brain injury. J. Neurosurg. 114, 92–101. https://doi.org/10.3171/2010.6.JNS10207

Ikezu, T., Ueda, H., Trapp, B.D., Nishiyama, K., Sha, J.F., Volonte, D., Galbiati, F., Byrd, A.L., Bassell, G., Serizawa, H., Lane, W.S., Lisanti, M.P., Okamoto, T., 1998. Affinity-purification and characterization of caveolins from the brain: Differential expression of caveolin-1, -2, and -3 in brain endothelial and astroglial cell types. Brain Res. 804, 177–192. https://doi.org/10.1016/S0006-8993(98)00498-3

Jeanne, M., Jorgensen, J., Gould, D.B., 2015. Molecular and Genetic Analyses of Collagen Type IV Mutant Mouse Models of Spontaneous Intracerebral Hemorrhage Identify Mechanisms for Stroke Prevention. Circulation 131, 1555–1565. https://doi.org/10.1161/CIRCULATIONAHA.114.013395

Liebner, S., Dijkhuizen, R.M., Reiss, Y., Plate, K.H., Agalliu, D., Constantin, G., 2018. Functional morphology of the blood-brain barrier in health and disease. Acta Neuropathol. (Berl.) 135, 311–336. https://doi.org/10.1007/s00401-018-1815-1

Lorenz, B., Garcia-Segura, L.M., DonCarlos, L.L., 2005. Cellular phenotype of androgen receptor-immunoreactive nuclei in the developing and adult rat brain. J. Comp. Neurol. 492, 456–468. https://doi.org/10.1002/cne.20763

Lu, M.L., Schneider, M.C., Zheng, Y., Zhang, X., Richie, J.P., 2001. Caveolin-1 interacts with androgen receptor. A positive modulator of androgen receptor mediated transactivation. J. Biol. Chem. 276, 13442–13451. https://doi.org/10.1074/jbc.M006598200

Martine, B., Marie-Jeanne, T., Cendrine, D., Fabrice, A., Marc, C., 2013. Assessment of Adult Human Exposure to Phthalate Esters in the Urban Centre of Paris (France). Bull. Environ. Contam. Toxicol. 90, 91–96. https://doi.org/10.1007/s00128-012-0859-5

Mhaouty-Kodja, S., 2018. Role of the androgen receptor in the central nervous system. Mol. Cell. Endocrinol., Androgens – revisiting their role as pleiotropic regulators of tissue function beyond the male reproductive system 465, 103–112. https://doi.org/10.1016/j.mce.2017.08.001

Mhaouty-Kodja, S., Naulé, L., Capela, D., 2018. Sexual Behavior: From Hormonal Regulation to Endocrine Disruption. Neuroendocrinology 107, 400–416. https://doi.org/10.1159/000494558

Montanaro, F., Carbonetto, S., 2003. Targeting Dystroglycan in the Brain. Neuron 37, 193–196. https://doi.org/10.1016/S0896-6273(03)00032-1

Noe, C.R., Noe-Letschnig, M., Handschuh, P., Noe, C.A., Lanzenberger, R., 2020. Dysfunction of the Blood-Brain Barrier-A Key Step in Neurodegeneration and Dementia. Front. Aging Neurosci. 12, 185. https://doi.org/10.3389/fnagi.2020.00185

Noell, S., Wolburg-Buchholz, K., Mack, A.F., Beedle, A.M., Satz, J.S., Campbell, K.P., Wolburg, H., Fallier-Becker, P., 2011. Evidence for a role of dystroglycan regulating the membrane architecture of astroglial endfeet. Eur. J. Neurosci. 33, 2179–2186. https://doi.org/10.1111/j.1460-9568.2011.07688.x

Palmer, A.M., 2011. The Role of the Blood Brain Barrier in Neurodegenerative Disorders and their Treatment. J. Alzheimers Dis. 24, 643–656. https://doi.org/10.3233/JAD-2011-110368

Patchev, V.K., Schroeder, J., Goetz, F., Rohde, W., Patchev, A.V., 2004. Neurotropic action of androgens: principles, mechanisms and novel targets. Exp. Gerontol. 39, 1651–1660. https://doi.org/10.1016/j.exger.2004.07.011

Rattan, S., Zhou, C., Chiang, C., Mahalingam, S., Brehm, E., Flaws, J.A., 2017. Exposure to endocrine disruptors during adulthood: consequences for female fertility. J Endocrinol. 233, 109-129. https://doi.org/10.1530/JOE-17-0023

Rempe, R.G., Hartz, A.M., Bauer, B., 2016. Matrix metalloproteinases in the brain and blood–brain barrier: Versatile breakers and makers. J. Cereb. Blood Flow Metab. 36, 1481–1507. https://doi.org/10.1177/0271678X16655551

Saha, R.N., Pahan, K., 2006. Signals for the induction of nitric oxide synthase in astrocytes. Neurochem. Int. 49, 154–163. https://doi.org/10.1016/j.neuint.2006.04.007

Sandoval, K.E., Witt, K.A., 2011. Age and 17β-estradiol effects on blood-brain barrier tight junction and estrogen receptor proteins in ovariectomized rats. Microvasc. Res. 81, 198–205. https://doi.org/10.1016/j.mvr.2010.12.007

Sharma, P., Ghavami, S., Stelmack, G.L., McNeill, K.D., Mutawe, M.M., Klonisch, T., Unruh, H., Halayko, A.J., 2010. β-Dystroglycan binds caveolin-1 in smooth muscle: a functional role in caveolae distribution and Ca2+ release. J. Cell Sci. 123, 3061–3070. https://doi.org/10.1242/jcs.066712

Shu, H., Zheng, G., Wang, X., Sun, Y., Liu, Y., Weaver, J.M., Shen, X., Liu, W., Jin, X., 2015. Activation of matrix metalloproteinase in dorsal hippocampus drives improvement in spatial working memory after intra-VTA nicotine infusion in rats. J. Neurochem. 135, 357–367. https://doi.org/10.1111/jnc.13283

Sofroniew, M.V., Vinters, H.V., 2010. Astrocytes: biology and pathology. Acta Neuropathol. (Berl.) 119, 7–35. https://doi.org/10.1007/s00401-009-0619-8

Sweeney, M.D., Sagare, A.P., Zlokovic, B.V., 2018. Blood-brain barrier breakdown in Alzheimer disease and other neurodegenerative disorders. Nat. Rev. Neurol. 14, 133–150. https://doi.org/10.1038/nrneurol.2017.188

Thomsen, M.S., Routhe, L.J., Moos, T., 2017. The vascular basement membrane in the healthy and pathological brain. J. Cereb. Blood Flow Metab. Off. J. Int. Soc. Cereb. Blood Flow Metab. 37, 3300–3317. https://doi.org/10.1177/0271678X17722436

Wolburg, H., Noell, S., Mack, A., Wolburg-Buchholz, K., Fallier-Becker, P., 2009. Brain endothelial cells and the glio-vascular complex. Cell Tissue Res. 335, 75–96. https://doi.org/10.1007/s00441-008-0658-9

Zaccaria, M.L., Di Tommaso, F., Brancaccio, A., Paggi, P., Petrucci, T.C., 2001. Dystroglycan distribution in adult mouse brain: a light and electron microscopy study. Neuroscience 104, 311–324. https://doi.org/10.1016/S0306-4522(01)00092-6

Zhang, X., Gu, Y., Li, P., Jiang, A., Sheng, X., Jin, X., Shi, Y., Li, G., 2019. Matrix Metalloproteases-Mediated Cleavage on β-Dystroglycan May Play a Key Role in the Blood–Brain Barrier After Intracerebral Hemorrhage in Rats. Med. Sci. Monit. Int. Med. J. Exp. Clin. Res. 25, 794–800. https://doi.org/10.12659/MSM.908500

Zlatnik, M.G., 2016. Endocrine-Disrupting Chemicals & Reproductive Health. J. Midwifery Womens Health 61, 442–455. https://doi.org/10.1111/jmwh.12500

Zlokovic, B.V., 2008. The Blood-Brain Barrier in Health and Chronic Neurodegenerative Disorders. Neuron 57, 178–201. https://doi.org/10.1016/j.neuron.2008.01.003

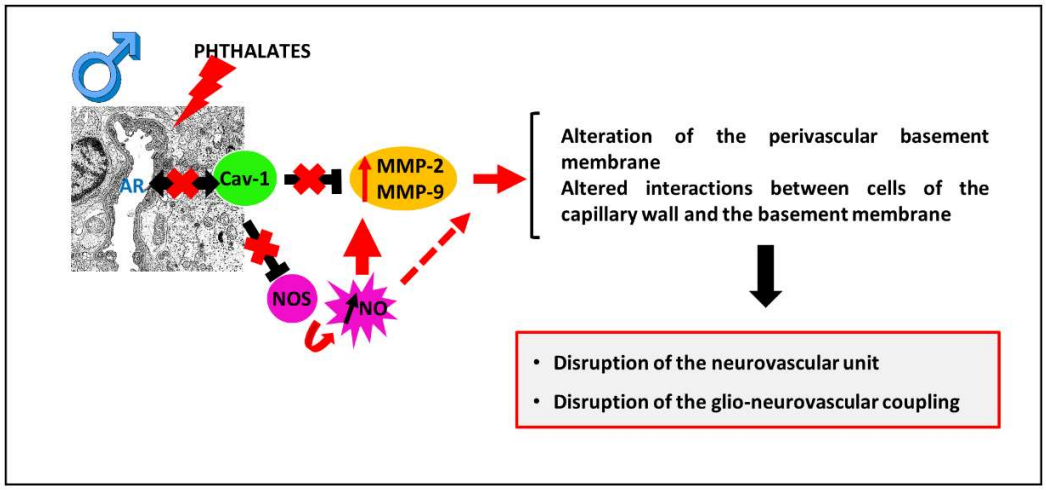

Graphical abstract: Proposed cellular pathway for glio-neurovascular coupling impairment in the mPOA of male mice following adult male mice exposure to low doses of DEHP alone or in an environmental phthalate mixture.
Adult exposure to DEHP alone or in mixture induces a decreased interaction between AR and Cav-1 protein in brain capillaries, leading to the activation of gelatinases which, in turn, generate alteration of the basement membrane and of cell-matrix interactions. This could result in a disruption of the glio-neurovascular unit and neuronal damages. The lower AR / Cav-1 interaction would also lead to an excessive amount of NO produced following phthalate-induced disinhibition of iNOS in astrocyte end-feet associated with capillaries. This proposed mode of action involving an AR-mediated cellular pathway could be involved in the adverse effects induced by phthalates on BBB integrity, thereby resulting in several alterations including the modifications previously reported for sexual behavior.